Available on: https://gjefm.ep-journals.org/ E-ISSN: 3117-6771, P-ISSN: 3117-6763

Global Journal of Education, Finance and Management

Volume: 02 Issue: 11 November 2026

# GPS-Based Identification of Traffic Bottlenecks and Buffer Time Estimation for Operational Risk Management in Port-Bound Container Drayage

**Ha Thi Huong**

Faculty of Economics, Hanoi Industrial and Trade University, Hanoi, Vietnam

**Published Date: November 26, 2026** **DOI: 10.65150/EP-gjefm/V2E11/2026-09**

**ABSTRACT:** Missing the container yard (CY) cut-off is one of the most costly operational risks in port-bound drayage, yet truck departures are often planned from average travel times and fixed rules of thumb. This study develops a framework that integrates Global Positioning System (GPS) probe data from truck telematics with the ISO 31000 risk management process to identify traffic bottlenecks and quantify the buffer time needed for reliable delivery to the port. A stylised 105.5 km corridor of 12 segments was simulated with 4,800 truck trips over 120 days and 1.26 million GPS pings, including positioning noise, missing pings, outliers, rest stops and gate dwell. The pipeline combined map matching, outlier filtering, stop detection, segment travel time extraction and geofencing with travel time reliability indicators, a space–time congestion map, counterfactual risk attribution and an expected-cost model for departure planning. Trip driving times were reproduced with a mean absolute percentage error of 0.23%. Two urban segments accounted for 72.6% of corridor delay, with planning time indices of up to 4.4 in the peaks. The 95th-percentile door-to-gate time ranged from 2.0 h at night to 3.7 h for afternoon departures, implying buffer times of 15 to 62 minutes above the mean, driven mainly by recurrent congestion and gate surges. For a 17:00 cut-off, the cost-optimal lead time reduced the probability of missing the cut-off from 8.4% to 1.2% and expected cost per trip by 47.9% compared with a mean-plus-30-minute rule. The framework converts GPS data into quantified risk treatment decisions.

**KEYWORDS:** GPS probe data, travel time reliability, buffer time, traffic bottleneck, container drayage, port cut-off, logistics risk management, ISO 31000

## INTRODUCTION

Port-bound road haulage, commonly called container drayage, is the link that connects inland production sites with the maritime network. For export flows, the critical constraint is the container yard (CY) cut-off: the latest time at which a laden container must have passed the terminal gate in order to be loaded onto the scheduled vessel. A container that misses the cut-off is typically rolled over to the next sailing, which triggers re-booking fees, additional storage and demurrage, possible penalties under the sales contract and, in time-sensitive supply chains, lost sales. The risk is asymmetric: arriving early costs truck and driver time, whereas arriving late can cost an entire week of transit time. Drayage planning is therefore an exercise in operational risk management under travel time uncertainty.

Travel time on port corridors is highly variable. Recurrent congestion during morning and evening peaks, merging and lane-drop bottlenecks, traffic incidents, adverse weather and queues at terminal gates combine to produce travel time distributions with long right tails (Noland & Polak, 2002; van Lint et al., 2008). In many emerging economies, including Vietnam, container trucks share urban arterials with dense mixed traffic, and gate operations at terminals are subject to surges as cut-off approaches. Planners who schedule departures on the basis of average travel time, or who add a fixed margin of 30 to 60 minutes regardless of departure time, are implicitly accepting an unknown and time-varying probability of failure.

At the same time, the information needed to manage this risk is increasingly available. Most container trucks are now equipped with Global Positioning System (GPS) telematics, often because regulation requires journey monitoring devices or because fleet operators use them for tracking and fuel management. Each truck produces a trajectory of time-stamped positions that, when aggregated over many trips, describes how travel time on every road segment varies by time of day, day of week and weather. Trajectory data mining and map matching are well-established fields (Quddus et al., 2007; Newson & Krumm, 2009; Zheng, 2015), and travel time reliability indicators have been standardised in transport engineering practice (Lomax et al., 2003; Federal Highway Administration [FHWA], 2006). However, these tools are rarely connected explicitly to the risk management process that logistics operators are expected to follow, for example under ISO 31000 (International Organization for Standardization [ISO], 2018).

This study addresses that gap by developing and demonstrating a GPS-based framework for drayage risk management. It is guided by three research questions: (RQ1) How can raw GPS probe data from container trucks be processed into reliable segment-level and trip-level travel time statistics? (RQ2) Where and when do bottlenecks occur along a port corridor, and which risk sources contribute most to the buffer time that must be planned? (RQ3) How much buffer time, and which departure time, minimise the expected cost of meeting a CY cut-off?

License: This is an open access article under the CC BY 4.0 license: https://creativecommons.org/licenses/by/4.0/

The contribution is threefold. Methodologically, the paper integrates map matching, stop detection, geofencing and reliability indicators into a single pipeline whose accuracy is verified against known ground truth. Analytically, it combines bottleneck identification with a counterfactual attribution of buffer time to individual risk sources, which tells managers where risk treatment will be most effective. Practically, it replaces fixed rules of thumb with an expected-cost model that converts the travel time distribution into a departure time recommendation for any cut-off.

## LITERATURE REVIEW

### *Supply chain and logistics risk management*

Supply chain risk management (SCRM) distinguishes between disruption risks, which are rare but severe, and operational risks arising from everyday variability in supply, demand, processes and transport (Tang, 2006). Systematic reviews show that transport-related operational risk receives less attention than supplier and demand risk, even though it directly affects service levels (Ho et al., 2015). Christopher and Peck (2004) argued that resilience requires visibility of the network and the creation of buffers where variability is high. In risk science, there is broad agreement that risk should be described by both the consequences and the associated uncertainty, quantified where data allow (Aven, 2016). ISO 31000 provides a generic process of risk identification, analysis, evaluation, treatment, and monitoring and review (ISO, 2018). Applied to drayage, this process requires a quantitative description of the travel time distribution, criteria for acceptable risk such as a maximum probability of missing the cut-off, and treatment options such as departure scheduling, buffer time and gate appointments.

### *Travel time reliability and buffer time*

Transport engineering has developed a family of reliability indicators that describe the variability of travel time from the user's perspective. The travel time index (TTI) compares mean travel time with free-flow travel time; the planning time index (PTI) compares the 95th-percentile travel time with free-flow travel time; and the buffer time index (BTI) expresses the extra time, above the mean, that a traveller must allow to arrive on time on 95% of trips (Lomax et al., 2003; FHWA, 2006). Chen et al. (2003) showed that reliability measures derived from loop detector data capture service quality better than averages, and van Lint et al. (2008) demonstrated that measures based on percentiles and skewness reveal unreliability that variance-based measures miss. The economics of reliability is well studied for passenger travel (Noland & Polak, 2002), while Figliozzi (2010) showed that congestion increases commercial vehicle tour costs disproportionately when time windows are tight, a situation that is typical for port cut-offs.

### *GPS probe data and bottleneck identification*

GPS-equipped vehicles act as probes that sample traffic conditions along their routes. Raw positions contain errors of several metres, occasional multipath outliers and gaps, so they must be map-matched to the road network before travel times can be computed (Quddus et al., 2007; Kaplan & Hegarty, 2017). Hidden Markov model approaches provide robust matching for sparse and noisy data (Newson & Krumm, 2009), and trajectory data mining techniques support stop detection, segmentation and pattern discovery (Zheng, 2015). Traffic flow theory explains bottlenecks as locations where capacity drops, for example at merges, lane drops and signalised junctions, causing queues that propagate upstream (Daganzo, 1997; Bertini & Leal, 2005). Probe data allow such bottlenecks to be located and characterised in space and time without fixed detectors.

### *Port gate congestion and drayage planning*

Terminal gates are recognised as a major source of delay and emissions in drayage. Truck appointment systems have been introduced at many ports to smooth arrivals (Giuliano & O'Brien, 2007; Huynh et al., 2016), and optimisation models have been proposed to set time windows that reduce gate queues (Chen et al., 2013). These studies focus on the terminal side, while the road segment of the journey is usually represented by a fixed or average travel time. Conversely, reliability studies of road corridors rarely include the gate dwell or the cut-off decision.

### *Research gap*

The literature therefore offers mature components but few integrated applications. First, GPS-based reliability analysis is seldom connected to a formal risk management process for logistics operations. Second, bottleneck studies identify where congestion occurs but rarely quantify how much each risk source contributes to the buffer time that a shipper must plan. Third, departure planning for port cut-offs is commonly based on average travel times, and the cost trade-off between early and late arrival is not made explicit. This study integrates these elements in one framework and evaluates it under controlled conditions in which the true travel times are known.

## MATERIALS AND METHODS

### *Research design and framework*

The study uses a design-science approach: a framework is constructed and then evaluated through a computational experiment. The framework maps the ISO 31000 process onto GPS data analytics in five stages. Risk identification uses GPS trajectories to detect where and when delays occur. Risk analysis estimates segment-level and trip-level travel time distributions and reliability indicators. Risk evaluation compares the probability of missing the cut-off with an acceptance criterion. Risk treatment selects departure times and buffer times that minimise expected cost. Monitoring and review update the statistics as new trajectories arrive. A simulation-based evaluation was chosen because it provides ground truth against which the accuracy of GPS processing can be verified, and because risk sources can be switched off one at a time, which is impossible with field data. All computations were implemented in Python 3 with NumPy and SciPy, with fixed random seeds for reproducibility.

### *Corridor and traffic model*

A stylised 105.5 km corridor was defined from an inland industrial park to a container terminal, representative of corridors linking industrial zones with seaports in northern Vietnam but not calibrated to any specific road. It consists of 12 segments of different types (Table 1). Segment speed was modelled with a Bureau of Public Roads (BPR)-type volume–delay function:

$$v_s(t) = v_{f,s} / [1 + \alpha \cdot x_s(t)^{\beta}] \cdot 1/\eta_{k,s}, \quad x_s(t) = \rho_s \cdot D(t) \cdot W_d \cdot \Omega(t) \cdot \Lambda_s(t) \tag{1}$$

where $v_{f,s}$ is the free-flow speed, $\rho_s$ the peak volume-to-capacity ratio of segment s, D(t) a time-of-day demand profile with morning (07:30) and evening (17:30) peaks, $W_d$ a day-of-week factor (1.00 on weekdays, 0.85 on Saturdays and 0.70 on Sundays), $\Omega(t)$ a weather factor (capacity reduced by 15% on rainy days, which occurred with probability 0.25), and $\Lambda_s(t)$ an incident factor (capacity reduced by 45% during incidents,

License: This is an open access article under the CC BY 4.0 license: https://creativecommons.org/licenses/by/4.0/

generated as a Poisson process with 0.012 incidents per km per day plus 0.05 per day at four high-risk segments, with a mean duration of one hour). The parameters were set to $\alpha = 0.8$ and $\beta = 5$, and speed was bounded below at 4 km/h. The term $\eta_{k,s}$, drawn from a lognormal distribution with $\sigma = 0.08$, represents heterogeneity between trucks and drivers. At the terminal, gate dwell (queue plus transaction) followed a lognormal distribution whose median varied from 12 minutes off-peak to 34 minutes around 16:00, with a 3% probability of a system slowdown adding 30 to 90 minutes. In addition, 8% of trips included a driver rest stop of 15 to 40 minutes in the rest area on segment S6.

**Table 1. Corridor segments and free-flow characteristics**

| Segment | Type | Length (km) | Free-flow speed (km/h) | Free-flow time (min) | Peak v/c ratio ρ |
|---|---|---|---|---|---|
| S1 | Industrial park access road | 3.0 | 40 | 4.5 | 0.60 |
| S2 | Provincial arterial (mixed traffic) | 8.0 | 50 | 9.6 | 1.15 |
| S3 | Interchange on-ramp (merge) | 1.5 | 40 | 2.2 | 1.10 |
| S4 | Expressway section 1 | 25.0 | 90 | 16.7 | 0.70 |
| S5 | Toll plaza | 0.8 | 30 | 1.6 | 0.95 |
| S6 | Expressway section 2 (rest area) | 30.0 | 90 | 20.0 | 0.65 |
| S7 | Bridge approach (lane drop) | 2.0 | 60 | 2.0 | 1.05 |
| S8 | Expressway section 3 | 20.0 | 90 | 13.3 | 0.70 |
| S9 | Exit ramp and signalised junction | 1.2 | 35 | 2.1 | 0.95 |
| S10 | Urban port road | 9.0 | 45 | 12.0 | 1.25 |
| S11 | Port access road | 4.0 | 40 | 6.0 | 0.90 |
| S12 | Terminal gate approach | 1.0 | 20 | 3.0 | 0.80 |
| Total | | 105.5 | | 93.0 | |

**Note: stylised corridor; parameters are model assumptions, not measurements of a specific road.**

***GPS data generation***

Over 120 days, 40 export trips per day were generated, with departure times distributed over 24 hours and concentrated between 05:00 and 20:00. Truck movement was simulated in 5-second steps, and each truck reported a GPS position every 30 seconds, which is a common logging interval for fleet telematics. Reported positions were perturbed by Gaussian noise with a standard deviation of 8 m in each horizontal coordinate. In addition, 2% of pings were randomly dropped, and 0.3% were displaced by about 150 m to emulate multipath errors in urban canyons. Trucks also reported positions while queuing inside the terminal gate area. In total, the dataset contained 1,256,004 pings from 4,800 trips. The true segment entry and exit times, gate dwell and rest stops were stored separately as ground truth and were not used by the processing pipeline.

***GPS processing pipeline***

The pipeline consisted of five steps. First, each ping was map-matched to the corridor centreline by nearest-point projection onto a polyline densified at 5 m spacing, using a k-d tree for efficiency. Second, pings farther than 40 m from the road or implying a speed above 130 km/h were removed as outliers, and the matched chainage $c_i$ was constrained to be non-decreasing along the trip, which is appropriate for a one-directional corridor:

$$c_i = \max(\, c_{i-1}, \operatorname{argmin}_c \| p_i - r(c) \| \,), \quad \text{subject to } \min_c \| p_i - r(c) \| \le 40 \text{ m} \tag{2}$$

where $p_i$ is the reported position and $r(c)$ the road geometry at chainage $c$. Third, stationary episodes lasting at least 10 minutes with a displacement of less than 50 m outside the gate geofence were classified as rest stops and excluded from driving time. Fourth, the time at which each truck crossed each segment boundary $C_j$ was obtained by linear interpolation between consecutive pings:

$$t(C_j) = t_i + (C_j - c_i)\cdot(t_{i+1} - t_i) / (c_{i+1} - c_i), \quad c_i \le C_j < c_{i+1} \tag{3}$$

Fifth, gate dwell was measured with a circular geofence of 150 m radius around the terminal gate, as the time between the first and the last ping inside the geofence. Door-to-gate time was defined as driving time plus gate dwell.

***Reliability indicators and bottleneck identification***

For each segment and time period, travel times were grouped by the time at which trucks entered the segment, so that congestion was attributed to the correct hour. The following indicators were computed:

$$\mathrm{TTI} = \bar{T} / t_{ff}, \quad \mathrm{PTI} = T_{95} / t_{ff}, \quad \mathrm{BTI} = (T_{95} - \bar{T}) / \bar{T}, \quad \mathrm{CF} = \Pr(\, v / v_f < 0.5 \,) \tag{4}$$

where $\bar{T}$ is the mean travel time, $T_{95}$ the 95th-percentile travel time, $t_{ff}$ the free-flow travel time and CF the congestion frequency, defined as the share of traversals at less than half the free-flow speed. A space–time congestion map was produced from the median speed ratio of each segment in each hour. Segments were ranked as bottlenecks by their mean delay per trip, $D_s = E[T_s - t_{ff,s}]$, and by their share of total corridor delay, with the delay intensity per km and the reliability indicators used to distinguish primary from secondary bottlenecks.

***Buffer time, risk attribution and departure planning***

At trip level, the buffer time for departure hour $h$ was defined, following FHWA (2006), as the difference between the 95th-percentile and the mean door-to-gate time:

$$B_{95}(h) = T_{95}(h) - \bar{T}(h) \tag{5}$$

To attribute the buffer to risk sources, the simulation was re-run five times with common random numbers, each time removing one source: recurrent (time-of-day) congestion, traffic incidents, adverse weather, time-of-day variation in gate dwell, and truck/driver heterogeneity. The reduction in the 95th-percentile time relative to the baseline measures the contribution of that source. Because the effects interact, contributions are not strictly additive.

License: This is an open access article under the CC BY 4.0 license: https://creativecommons.org/licenses/by/4.0/

For departure planning, let C be the CY cut-off and $\Lambda$ the planned lead time, so that the truck departs at $C - \Lambda$. With door-to-gate time T conditional on that departure time, the expected cost per trip is

$$EC(\Lambda) = c_L \cdot Pr(T > \Lambda) + c_E \cdot E[\,(\Lambda - T)^+\,] \quad (6)$$

where $c_L$ is the cost of missing the cut-off and $c_E$ the cost per hour of early arrival (truck and driver waiting time). The conditional distribution of T was estimated empirically from GPS-derived trips departing within ±30 minutes of $C - \Lambda$. Illustrative values of $c_L$ = USD 250 per container and $c_E$ = USD 12 per hour were used; these are model parameters, and a sensitivity analysis was performed for $c_L$ between USD 100 and USD 1,000. Three policies were compared for cut-offs at 11:00, 17:00 and 23:00: a rule of thumb (mean travel time plus 30 minutes), a 95th-percentile rule ($\Lambda = T_{95}$), and the cost-optimal lead time obtained by minimising Equation (6) over a 3-minute grid.

## RESULTS

### *Accuracy of the GPS processing pipeline*

Table 2 summarises data quality and the accuracy of the estimates against ground truth. Of the 1,256,004 pings, 25,240 (2.0%) were missing and 2,961 (0.24%) were removed as outliers, leaving 1,227,803 valid pings. The stop-detection rule identified 386 stationary episodes, compared with 382 actual rest stops. Trip driving time was reproduced with a mean absolute percentage error (MAPE) of 0.23% and a correlation of 0.9999 with the true value. Segment travel times had a MAPE of 0.2% to 3.2% for segments of 1.2 km or more, and 8.5% to 8.9% for the two shortest segments (S5, 0.8 km; S12, 1.0 km), whose traversal times were close to the 30-second logging interval. Gate dwell measured by the geofence had a mean absolute error of 0.27 minutes.

**Table 2. Data quality and accuracy of GPS-derived travel times against ground truth**

| Indicator | Value |
|---|---|
| Trips / observation days | 4,800 / 120 |
| GPS pings generated (30 s interval) | 1,256,004 |
| Missing pings | 25,240 (2.0%) |
| Outliers removed (>40 m from road or >130 km/h) | 2,961 (0.24%) |
| Valid pings after cleaning | 1,227,803 |
| Rest stops: detected / actual | 386 / 382 |
| MAPE of trip driving time | 0.23% (r = 0.9999) |
| MAPE of segment travel time, segments ≥ 1.2 km | 0.2–3.2% |
| MAPE of segment travel time, S5 (0.8 km) and S12 (1.0 km) | 8.9% and 8.5% |
| Mean absolute error of gate dwell (geofence 150 m) | 0.27 min |

### *Space–time congestion pattern*

Figure 1 shows the space–time congestion map derived from the GPS data. Two congestion regimes are evident. In the morning peak (06:00–09:00) and, more severely, in the evening peak (15:00–19:00), median speeds on the provincial arterial (S2) and the urban port road (S10) fell to 31–46% of free-flow speed. The interchange merge (S3) and the bridge lane drop (S7) slowed to 42–55% and 51–61% of free-flow speed at the same hours, while the expressway sections (S4, S6, S8) remained near free-flow speed throughout the day. Between 09:00 and 15:00, S2 and S10 operated at 80–91% of free-flow speed, and night conditions were close to free flow on all segments.

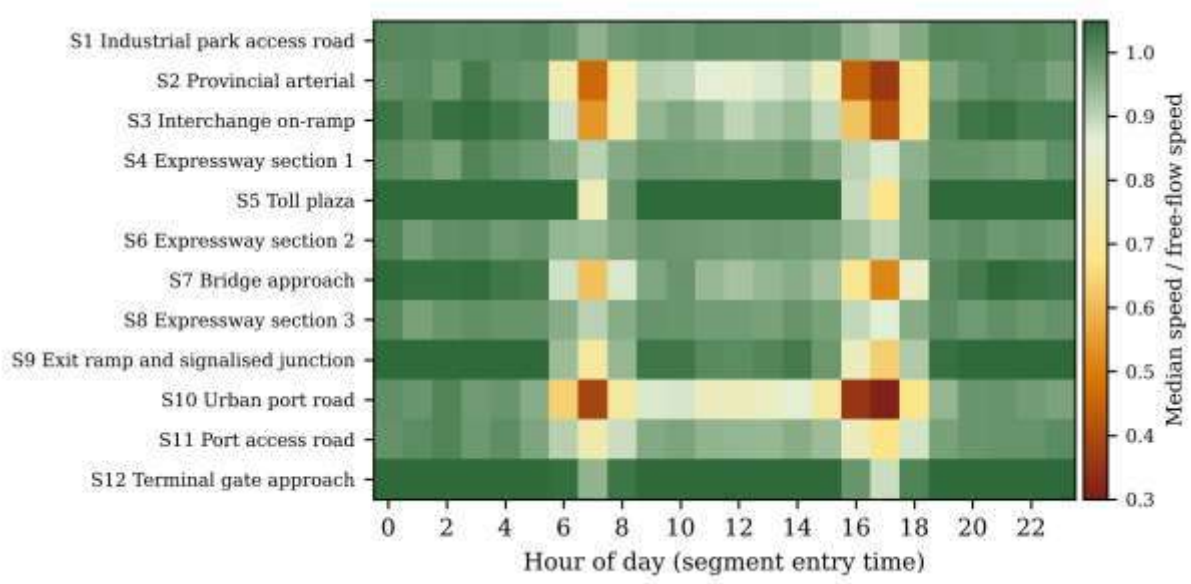


**Figure 1. Space–time congestion map: median speed ratio by segment and hour of segment entry (GPS-derived)**

License: This is an open access article under the CC BY 4.0 license: https://creativecommons.org/licenses/by/4.0/

***Segment reliability and bottleneck ranking***

Table 3 reports reliability indicators by segment. The mean delay per trip over the whole corridor was 13.1 minutes relative to free flow. The urban port road S10 contributed 5.6 minutes (42.6%) and the provincial arterial S2 contributed 3.9 minutes (30.0%), together accounting for 72.6% of total delay. Both segments had the highest delay intensity (0.62 and 0.49 min per km), congestion frequencies of 27.4–39.5% in the peaks, and planning time indices of 4.37–4.43 (S10) and 3.47–4.39 (S2). The interchange merge S3 had high relative unreliability (PTI 3.08 and CF 27.2% in the evening peak) but a small absolute delay because of its short length. The bridge lane drop S7 showed similar but weaker behaviour. The expressway sections had TTI values of 1.04–1.05 and BTI values of 0.15–0.16 over the day.

**Table 3. Segment reliability indicators and bottleneck ranking (GPS-derived)**

| Segment | Mean delay (min/trip) | Share of delay (%) | Delay per km (min) | TTI all day | PTI all day | BTI all day | TTI PM peak | PTI PM peak | CF PM peak (%) | Rank |
|---|---|---|---|---|---|---|---|---|---|---|
| S10 Urban port road | 5.60 | 42.6 | 0.62 | 1.47 | 3.29 | 1.24 | 2.21 | 4.37 | 39.5 | 1 |
| S2 Provincial arterial | 3.94 | 30.0 | 0.49 | 1.41 | 2.91 | 1.06 | 2.04 | 4.39 | 37.8 | 2 |
| S3 Interchange merge | 0.59 | 4.5 | 0.39 | 1.26 | 2.34 | 0.85 | 1.70 | 3.08 | 27.2 | 3 |
| S7 Bridge lane drop | 0.30 | 2.3 | 0.15 | 1.15 | 1.82 | 0.58 | 1.45 | 2.50 | 12.6 | 4 |
| S11 Port access road | 0.58 | 4.4 | 0.14 | 1.10 | 1.44 | 0.31 | 1.24 | 1.72 | 2.2 | 5 |
| S9 Exit ramp/junction | 0.11 | 0.8 | 0.09 | 1.05 | 1.49 | 0.42 | 1.24 | 1.88 | 3.9 | 6 |
| S4 Expressway 1 | 0.82 | 6.2 | 0.03 | 1.05 | 1.22 | 0.16 | 1.10 | 1.31 | 0.3 | – |
| S6 Expressway 2 | 0.74 | 5.7 | 0.02 | 1.04 | 1.19 | 0.15 | 1.08 | 1.26 | 0.6 | – |
| S8 Expressway 3 | 0.57 | 4.3 | 0.03 | 1.04 | 1.21 | 0.16 | 1.10 | 1.31 | 0.8 | – |
| S5 Toll plaza | −0.03 | −0.2 | −0.04 | 0.98 | 1.41 | 0.44 | 1.16 | 1.81 | 3.8 | – |
| S1 Access road | 0.08 | 0.6 | 0.03 | 1.02 | 1.17 | 0.15 | 1.05 | 1.20 | 0.0 | – |
| S12 Gate approach | −0.15 | −1.2 | −0.15 | 0.95 | 1.17 | 0.23 | 1.01 | 1.27 | 0.0 | – |

**Note: PM peak = segment entry between 15:00 and 19:00; CF = share of traversals below 50% of free-flow speed. Ranking by delay per km among segments with positive mean delay and CF > 2% in the PM peak. Small negative delays arise because individual trucks may exceed the nominal free-flow speed and because the S12 boundary is set at the geofence edge.**

***Trip-level travel time and buffer time***

Figure 2 and Table 4 present door-to-gate times by departure hour. The overall mean was 128 minutes (2.14 h), compared with 93 minutes of free-flow driving plus 12 minutes of uncongested gate dwell, and the overall 95th percentile was 185 minutes (3.09 h). Both the level and the spread varied strongly with departure time. For departures between 20:00 and 02:00, the mean was 1.78–1.82 h and the buffer time was 15–20 minutes. For departures between 14:00 and 18:00, the mean rose to 2.62–2.67 h, the 95th percentile to 3.56–3.65 h and the buffer to 53–62 minutes, with a PTI of 2.03–2.09. Gate dwell contributed substantially to this pattern: the mean dwell rose from 13.7 minutes for midnight departures to 34.6–34.9 minutes for afternoon departures, and its 95th percentile reached 75–78 minutes.

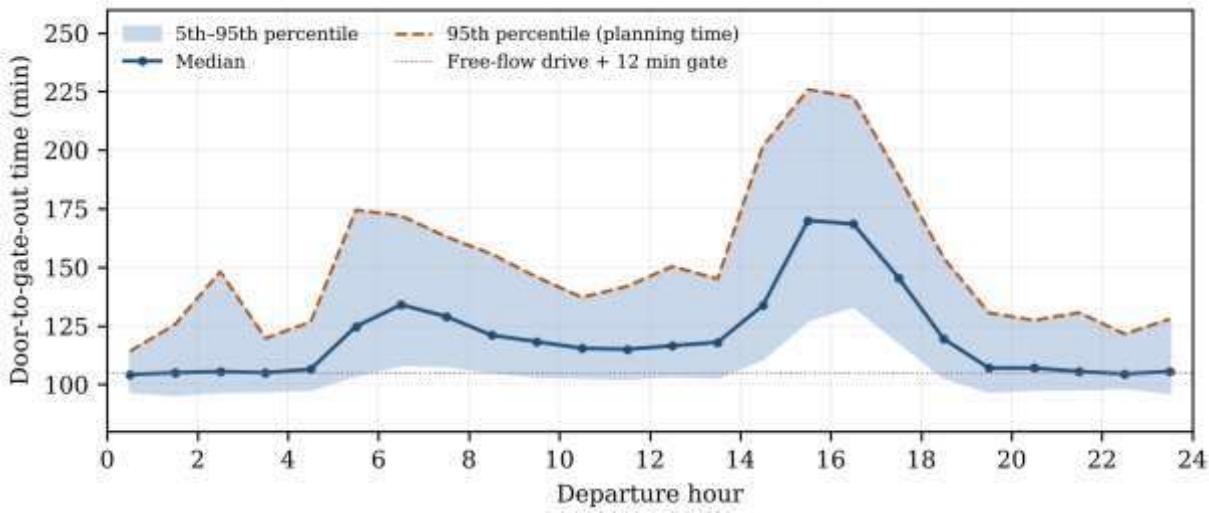


**Figure 2. Door-to-gate time by departure hour: median, 95th percentile and 5th–95th percentile band (GPS-derived)**

**Table 4. Door-to-gate time and buffer time by departure period**

| Departure | Trips | Mean (h) | Median (h) | 95th pct. (h) | Buffer (min) | $B_{95}$ | PTI | Mean gate dwell (min) | 95th pct. gate dwell (min) |
|---|---|---|---|---|---|---|---|---|---|
| 00:00–02:00 | 114 | 1.78 | 1.74 | 2.03 | 15 | | 1.16 | 13.7 | 30.5 |
| 02:00–04:00 | 82 | 1.82 | 1.75 | 2.34 | 32 | | 1.34 | 15.9 | 45.4 |

License: This is an open access article under the CC BY 4.0 license: https://creativecommons.org/licenses/by/4.0/

| Departure | Trips | Mean (h) | Median (h) | 95th pct. (h) | Buffer $B_{95}$ (min) | PTI | Mean gate dwell (min) | 95th pct. gate dwell (min) |
|---|---|---|---|---|---|---|---|---|
| 04:00–06:00 | 416 | 2.05 | 1.94 | 2.79 | 44 | 1.60 | 15.6 | 33.6 |
| 06:00–08:00 | 535 | 2.24 | 2.20 | 2.82 | 35 | 1.61 | 17.1 | 35.7 |
| 08:00–10:00 | 511 | 2.04 | 1.99 | 2.50 | 27 | 1.43 | 23.6 | 50.0 |
| 10:00–12:00 | 547 | 1.97 | 1.92 | 2.35 | 23 | 1.34 | 18.4 | 41.1 |
| 12:00–14:00 | 551 | 2.01 | 1.95 | 2.47 | 28 | 1.41 | 21.1 | 49.8 |
| 14:00–16:00 | 490 | 2.62 | 2.51 | 3.65 | 62 | 2.09 | 34.9 | 77.8 |
| 16:00–18:00 | 524 | 2.67 | 2.59 | 3.56 | 53 | 2.03 | 34.6 | 75.4 |
| 18:00–20:00 | 522 | 1.94 | 1.88 | 2.48 | 32 | 1.42 | 19.8 | 46.4 |
| 20:00–22:00 | 372 | 1.82 | 1.77 | 2.15 | 20 | 1.23 | 15.5 | 36.0 |
| 22:00–24:00 | 136 | 1.81 | 1.76 | 2.07 | 16 | 1.18 | 15.4 | 29.8 |

**Note: PTI relative to 105 min (free-flow driving plus 12 min gate dwell). Night periods have smaller samples, so their 95th percentiles are less precise.**

***Attribution of buffer time to risk sources***

Table 5 reports the counterfactual analysis. Removing recurrent congestion reduced the overall 95th-percentile time by 34.0 minutes and the buffer by 22.2 minutes; for afternoon departures (14:00–17:00), the reduction in the 95th percentile was 47.2 minutes. Removing time-of-day variation in gate dwell reduced the overall 95th percentile by 18.9 minutes and the afternoon 95th percentile by 28.4 minutes. Adverse weather contributed 8.7 minutes overall and 10.8 minutes in the afternoon. Traffic incidents and truck/driver heterogeneity contributed less than 3.0 minutes each at the 95th-percentile level.

**Table 5. Contribution of risk sources to door-to-gate time (counterfactual simulation, minutes)**

| Scenario | Mean (all) | 95th pct. (all) | Buffer (all) | Reduction of 95th pct. (all) | 95th pct. (14:00–17:00) | Reduction of 95th pct. (14:00–17:00) |
|---|---|---|---|---|---|---|
| Baseline (all risk sources) | 128.6 | 185.7 | 57.1 | – | 220.7 | – |
| Without recurrent congestion | 116.8 | 151.7 | 34.9 | 34.0 | 173.5 | 47.2 |
| Without gate time-of-day variation | 121.7 | 166.8 | 45.1 | 18.9 | 192.3 | 28.4 |
| Without adverse weather | 125.8 | 177.0 | 51.2 | 8.7 | 209.9 | 10.8 |
| Without traffic incidents | 128.0 | 184.7 | 56.6 | 1.0 | 217.7 | 3.0 |
| Without truck/driver heterogeneity | 128.2 | 185.2 | 57.0 | 0.5 | 219.3 | 1.4 |

**Note: common random numbers across scenarios; rest-stop time excluded. Contributions interact and are not strictly additive.**

***Departure planning for CY cut-offs***

Table 6 compares the three departure policies, and Figure 3 shows the expected cost curve for a 17:00 cut-off. For the 17:00 cut-off, the mean-plus-30-minute rule gave a lead time of 2.75 h (departure 14:15), a probability of missing the cut-off of 8.4% and an expected cost of USD 27.69 per trip. The 95th-percentile rule gave 2.90 h, 5.0% and USD 21.51. The cost-optimal lead time was 3.05 h (departure 13:57), with a probability of 1.2% and an expected cost of USD 14.42, which is 47.9% lower than the rule of thumb and 33.0% lower than the 95th-percentile rule. For the 11:00 cut-off, the optimal lead time of 3.35 h reduced expected cost by 18.5% compared with both rules, which coincided at 2.60 h. For the 23:00 cut-off, the rule of thumb coincided with the optimum (2.30 h, 2.0%), whereas the 95th-percentile rule produced a higher risk of 5.6%. In the sensitivity analysis for the 17:00 cut-off, the optimal lead time was 3.05 h for $c_L$ = USD 100 and USD 250 and 3.25 h for USD 500 and USD 1,000, with probabilities of missing the cut-off of 1.2% and 0.4%, respectively.

**Table 6. Comparison of departure policies for three CY cut-off times**

| Cut-off | Policy | Lead time Λ (h) | Departure | Pr(miss cut-off) (%) | Expected cost (USD/trip) | Change vs rule of thumb (%) |
|---|---|---|---|---|---|---|
| 11:00 | Mean + 30 min | 2.60 | 08:24 | 4.4 | 17.39 | – |
| 11:00 | 95th-percentile rule | 2.60 | 08:24 | 4.4 | 17.39 | 0.0 |
| 11:00 | Cost-optimal | 3.35 | 07:39 | 0.0 | 14.17 | −18.5 |
| 17:00 | Mean + 30 min | 2.75 | 14:15 | 8.4 | 27.69 | – |
| 17:00 | 95th-percentile rule | 2.90 | 14:06 | 5.0 | 21.51 | −22.3 |
| 17:00 | Cost-optimal | 3.05 | 13:57 | 1.2 | 14.42 | −47.9 |
| 23:00 | Mean + 30 min | 2.30 | 20:42 | 2.0 | 11.01 | – |
| 23:00 | 95th-percentile rule | 2.05 | 20:57 | 5.6 | 16.95 | +54.0 |
| 23:00 | Cost-optimal | 2.30 | 20:42 | 2.0 | 11.01 | 0.0 |

**Note: c_L = USD 250 per missed cut-off and c_E = USD 12 per hour of early arrival (illustrative). Probabilities are estimated from 180–280 GPS-derived trips per departure window; 0.0% means no late trip was observed in the sample.**

License: This is an open access article under the CC BY 4.0 license: https://creativecommons.org/licenses/by/4.0/

Corresponding Author: Ha Thi Huong

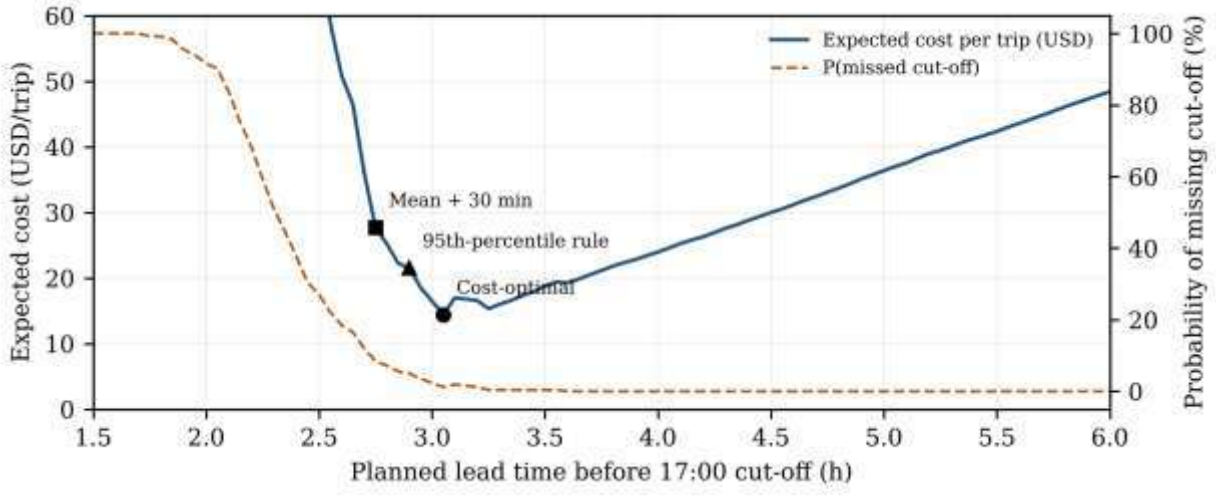


**Figure 3. Expected cost per trip and probability of missing a 17:00 cut-off as functions of the planned lead time**

## DISCUSSION

***GPS data as a basis for quantitative risk analysis***

The first research question concerned the processing of raw GPS data. The results show that a relatively simple pipeline of projection-based map matching, outlier filtering, stop detection and boundary interpolation recovers trip driving times almost exactly and segment travel times with errors that depend mainly on segment length relative to the logging interval. This is consistent with the map-matching literature, which identifies sampling interval and positioning error as the main determinants of accuracy (Quddus et al., 2007; Newson & Krumm, 2009). For practice, two implications follow. Segments shorter than about the distance travelled in two logging intervals should be merged or analysed with a higher logging frequency, and stop detection is essential, because unremoved rest stops would be misread as congestion and would inflate the estimated buffer. In real deployments with branching networks, more robust matching methods such as hidden Markov models are required, but the overall logic of the framework is unchanged.

***Where bottlenecks are and why they matter for risk***

The second research question concerned bottlenecks and risk sources. The space–time map and the ranking agree that delay on the corridor is concentrated in two urban segments at the ends of the route, while the expressway sections, which make up 71% of the length, contribute little to either delay or variability. This pattern is typical of port corridors in which high-capacity intercity roads feed into constrained urban roads near the port (Rodrigue, 2020). The merge and lane-drop segments behave as classical capacity bottlenecks (Daganzo, 1997; Bertini & Leal, 2005): they are short and therefore cause little absolute delay, but their high PTI shows that they can trigger queues and unreliability at peak times. A ranking based on mean delay alone would understate them, which supports the use of several reliability indicators together, as recommended by van Lint et al. (2008).

The counterfactual attribution adds an important managerial insight: at the 95th-percentile level, which is the level relevant for meeting a cut-off, the buffer is driven mainly by recurrent congestion and by gate surges, both of which are predictable by time of day. Incidents, although important for individual trips, rarely coincide with a given trip and therefore have only a small effect at the 95th percentile, although they shape the extreme tail beyond it. This means that a large part of what operators perceive as uncertainty is in fact predictable variability that can be avoided by shifting departure times, rather than risk that must be absorbed by a larger buffer. This finding is consistent with the observation by Figliozzi (2010) that the costs of congestion for commercial vehicles depend strongly on the timing of operations.

***From buffer time to risk treatment***

The third research question concerned departure planning. The expected-cost model shows that fixed rules of thumb are inconsistent across the day: the mean-plus-30-minute rule was adequate for a night cut-off but exposed 8.4% of trips to a missed cut-off for a 17:00 cut-off, because both the mean and the variance of travel time increase sharply for departures after about 14:00. The 95th-percentile rule, which is the logic behind the buffer time index (FHWA, 2006), performs better in the afternoon but is not cost-optimal, because it ignores the asymmetry between the cost of being late and the cost of waiting. The optimal solution for the 17:00 cut-off was not simply a larger buffer but an earlier departure that avoided the onset of evening congestion and the gate surge, which is why it was almost insensitive to the penalty cost between USD 100 and USD 250. This illustrates how the treatment stage of ISO 31000 can be made quantitative: the risk criterion, for example a maximum probability of 2% of missing the cut-off, and the cost trade-off can be evaluated explicitly and updated continuously as new GPS data arrive (Aven, 2016; ISO, 2018).

***Managerial and policy implications***

For logistics operators and freight forwarders, the framework suggests a practical procedure: collect GPS trajectories from their own fleet, compute the departure-time-dependent distribution of door-to-gate time, set an explicit risk criterion, and schedule departures by cut-off and day type rather than by a single fixed margin. Bottleneck rankings can be used to choose alternative routes or to negotiate time windows with customers. For terminal operators, the large contribution of gate surges indicates that truck appointment systems and extended gate hours would reduce the buffers required by all users (Giuliano & O'Brien, 2007; Huynh et al., 2016; Chen et al., 2013). For transport authorities, the concentration of delay on short urban segments near the port suggests that targeted capacity improvements, dedicated truck lanes or traffic signal coordination on these segments would yield larger reliability gains than further expansion of intercity expressways.

License: This is an open access article under the CC BY 4.0 license: https://creativecommons.org/licenses/by/4.0/

***Limitations***

The study has several limitations. First, the corridor, traffic parameters, gate model and costs are stylised assumptions rather than measurements of a specific road or terminal; the numerical results illustrate the framework and should not be interpreted as estimates for any real corridor. Validation with real telematics data from container fleets is the most important next step. Second, the corridor has a single route, so route choice and network effects are not considered, and the simple map-matching method would need to be replaced by a more robust algorithm for branching networks. Third, empirical percentiles were estimated from 180 to 280 trips per departure window, so small probabilities, especially zero observed lates, have considerable sampling uncertainty. Fourth, congestion was modelled with a static volume–delay function that does not represent queue spillback between segments. Fifth, the cost model considers only the early-waiting and cut-off penalties; driver hours-of-service regulations, truck utilisation and emissions were not included.

## CONCLUSION

This study developed and evaluated a framework that connects GPS probe data from container trucks with the ISO 31000 risk management process for port-bound drayage. Using a simulated corridor with known ground truth, it showed that GPS trajectories can be processed into accurate segment-level and trip-level travel time statistics, with a driving-time error of 0.23%. The analysis located the main bottlenecks on two urban segments that generated 72.6% of corridor delay, showed that the buffer time needed for 95% on-time arrival ranges from about 15 minutes at night to over one hour in the afternoon, and attributed most of this buffer to predictable recurrent congestion and terminal gate surges. An expected-cost model turned these statistics into departure recommendations that, for a 17:00 cut-off, reduced the probability of missing the cut-off from 8.4% to 1.2% and the expected cost per trip by almost half compared with a common rule of thumb.

The main contributions are an integrated and verifiable GPS processing pipeline, a counterfactual method for attributing buffer time to risk sources, and a cost-based departure planning rule that makes the risk treatment step explicit. Future research should apply the framework to real fleet telematics data on Vietnamese port corridors, combine it with real-time traffic and terminal information for dynamic re-planning, extend it to networks with alternative routes, and integrate it with truck appointment systems so that road and terminal reliability can be managed jointly. Policy makers and port authorities could support such applications by encouraging data sharing between trucking companies, terminals and traffic management centres.

## ACKNOWLEDGMENT

The author thanks colleagues at the Faculty of Electromechanical Engineering, Hanoi University of Industry and Trade, for their comments on the framework. This research received no specific grant from any funding agency in the public, commercial or not-for-profit sectors.

## ETHICAL AND COMPLIANCE STATEMENTS

**Plagiarism statement:** The author confirms that this manuscript is original and that the similarity index will not exceed 15%.

**Conflict of interest:** The author declares no conflict of interest.

**Funding:** This research received no external funding.

**Research ethics:** The study is based on simulated data and did not involve human participants, personal location data or animals; ethics approval was therefore not required.

**Data availability:** The simulation and processing code and parameters are available from the author on reasonable request.

## REFERENCES

1) Aven, T. (2016). Risk assessment and risk management: Review of recent advances on their foundation. European Journal of Operational Research, 253(1), 1–13. https://doi.org/10.1016/j.ejor.2015.12.023
2) Bertini, R. L., & Leal, M. T. (2005). Empirical study of traffic features at a freeway lane drop. Journal of Transportation Engineering, 131(6), 397–407.
3) Chen, C., Skabardonis, A., & Varaiya, P. (2003). Travel-time reliability as a measure of service. Transportation Research Record, 1855, 74–79. https://doi.org/10.3141/1855-09
4) Chen, G., Govindan, K., & Yang, Z. (2013). Managing truck arrivals with time windows to alleviate gate congestion at container terminals. International Journal of Production Economics, 141(1), 179–188. https://doi.org/10.1016/j.ijpe.2012.03.033
5) Christopher, M., & Peck, H. (2004). Building the resilient supply chain. The International Journal of Logistics Management, 15(2), 1–14. https://doi.org/10.1108/09574090410700275
6) Daganzo, C. F. (1997). Fundamentals of transportation and traffic operations. Pergamon.
7) Federal Highway Administration. (2006). Travel time reliability: Making it there on time, all the time (Report No. FHWA-HOP-06-070). U.S. Department of Transportation.
8) Figliozzi, M. A. (2010). The impacts of congestion on commercial vehicle tour characteristics and costs. Transportation Research Part E: Logistics and Transportation Review, 46(4), 496–506. https://doi.org/10.1016/j.tre.2009.04.005
9) Giuliano, G., & O'Brien, T. (2007). Reducing port-related truck emissions: The terminal gate appointment system at the Ports of Los Angeles and Long Beach. Transportation Research Part D: Transport and Environment, 12(7), 460–473. https://doi.org/10.1016/j.trd.2007.06.004
10) Ho, W., Zheng, T., Yildiz, H., & Talluri, S. (2015). Supply chain risk management: A literature review. International Journal of Production Research, 53(16), 5031–5069. https://doi.org/10.1080/00207543.2015.1030467
11) Huynh, N., Smith, D., & Harder, F. (2016). Truck appointment systems: Where we are and where to go from here. Transportation Research Record, 2548, 1–9. https://doi.org/10.3141/2548-01

License: This is an open access article under the CC BY 4.0 license: https://creativecommons.org/licenses/by/4.0/

Corresponding Author: Ha Thi Huong

12) International Organization for Standardization. (2018). ISO 31000:2018 Risk management – Guidelines. ISO.
13) Kaplan, E. D., & Hegarty, C. J. (Eds.). (2017). Understanding GPS/GNSS: Principles and applications (3rd ed.). Artech House.
14) Lomax, T., Schrank, D., Turner, S., & Margiotta, R. (2003). Selecting travel reliability measures. Texas Transportation Institute and Cambridge Systematics.
15) Newson, P., & Krumm, J. (2009). Hidden Markov map matching through noise and sparseness. In Proceedings of the 17th ACM SIGSPATIAL International Conference on Advances in Geographic Information Systems (pp. 336–343). ACM. https://doi.org/10.1145/1653771.1653818
16) Noland, R. B., & Polak, J. W. (2002). Travel time variability: A review of theoretical and empirical issues. Transport Reviews, 22(1), 39–54. https://doi.org/10.1080/01441640010022456
17) Quddus, M. A., Ochieng, W. Y., & Noland, R. B. (2007). Current map-matching algorithms for transport applications: State-of-the art and future research directions. Transportation Research Part C: Emerging Technologies, 15(5), 312–328. https://doi.org/10.1016/j.trc.2007.05.002
18) Rodrigue, J.-P. (2020). The geography of transport systems (5th ed.). Routledge.
19) Tang, C. S. (2006). Perspectives in supply chain risk management. International Journal of Production Economics, 103(2), 451–488. https://doi.org/10.1016/j.ijpe.2005.12.006
20) van Lint, J. W. C., van Zuylen, H. J., & Tu, H. (2008). Travel time unreliability on freeways: Why measures based on variance tell only half the story. Transportation Research Part A: Policy and Practice, 42(1), 258–277. https://doi.org/10.1016/j.tra.2007.08.008
21) Zheng, Y. (2015). Trajectory data mining: An overview. ACM Transactions on Intelligent Systems and Technology, 6(3), Article 29. https://doi.org/10.1145/2743025

License: This is an open access article under the CC BY 4.0 license: https://creativecommons.org/licenses/by/4.0/

Corresponding Author: Ha Thi Huong